SCIENTIFIC REPORTS

OPEN

Radicalization and Radical Catalysis of Biomass Sugars: Insights from First-principles Studies

Received: 14 February 2016
Accepted: 21 June 2016
Published: 13 July 2016

Gang Yang, Chang Zhu, Xianli Zou & Lijun Zhou

A*b initio* and density functional calculations are conducted to investigate the radicalization processes and radical catalysis of biomass sugars. Structural alterations due to radicalization generally focus on the radicalized sites, and radicalization affects H-bonds in D-fructofuranose more than in D-glucopyranose, potentially with outcome of new H-bonds. Performances of different functionals and basis sets are evaluated for all radicalization processes, and enthalpy changes and Gibbs free energies for these processes are presented with high accuracy, which can be referenced for subsequent experimental and theoretical studies. It shows that radicalization can be utilized for direct transformation of biomass sugars, and for each sugar, C rather than O sites are always preferred for radicalization, thus suggesting the possibility to activate C-H bonds of biomass sugars. Radical catalysis is further combined with Brønsted acids, and it clearly states that functionalization fundamentally regulates the catalytic effects of biomass sugars. In presence of explicit water molecules, functionalization significantly affects the activation barriers and reaction energies of protonation rather than dehydration steps. Tertiary butyl and phenyl groups with large steric hindrances or hydroxyl and amino groups resulting in high stabilities for protonation products drive the protonation steps to occur facilely at ambient conditions.

Petroleum resources are expected to be exhausted in the next few decades, and alternative energy sources are being sought. Owing to the abundance, sustainability and easy availability, cellulosic biomass has been regarded as a promising energy source to replace petroleum[1–3]; nonetheless, the direct transformation of cellulosic biomass to downstream products remains a grand challenge[4].

Glucose, the monomer of cellulose, has often been used as protype to investigate the transformation of cellulosic biomass[5–15]. The Brønsted-acid catalysis of glucose is driven towards the formation of humin precursors and reversion products, while under similar conditions, fructose can be activated readily and with a sequence of facile reaction steps converted to 5-(hydroxymethyl)furfural (HMF) or other platform chemicals[16–18]. Sn-BEA zeolite and HCl solutions were skilfully combined by Nikolla *et al.*[19], realizing the "one-pot" synthesis of HMF from glucose with relatively high conversion and selectivity. On the other hand, glucose has lower acidity than fructose[20–23] and hence is less reactive under basic conditions. Recently, Liu *et al.*[24] have demonstrated that organic amines are efficient for the isomerization of glucose to fructose. These clearly state that whether in acidic or basic environments, fructose acts as the pivotal intermediate for the transformation of cellulosic sugars.

In the past few decades, radical catalysis has emerged into a flourishing area[25,26], while reports relating to biomass transformations are scarce. Electron magnetic resonances were used to study the irradiation of crystalline D-glucose, D-fructose and sucrose[27–30], and several C-centered radicals were assigned with help of density functional calculations[30–32]. The radical stabilities can be expressed using the isodesmic H-transfer reactions[33,34],

$$RSE = E_r = E(A^{\bullet}) + E(CH_4) - E(A) - E(CH_3^{\bullet}) \quad (1)$$

Reaction enthalpy of Eq. 1 is also referred to as radical stabilization energy (*RSE*). The *RSE* calculations with acceptable accuracy allows for quantitative estimation of H-transfer reaction energies and optimization of the properties for new reagents[35]. A comprehensive understanding of C-centered sugar radicals is lacking, which was presently conducted with high-level *ab initio* calculations (MP2/aug-cc-pVTZ). D-glucose (monomer of

College of Resources and Environments & Chongqing Key Laboratory of Soil Multi-scale Interfacial Process, Southwest University, Chongqing 400715, China. Correspondence and requests for materials should be addressed to G.Y. (email: theobiochem@gmail.com)

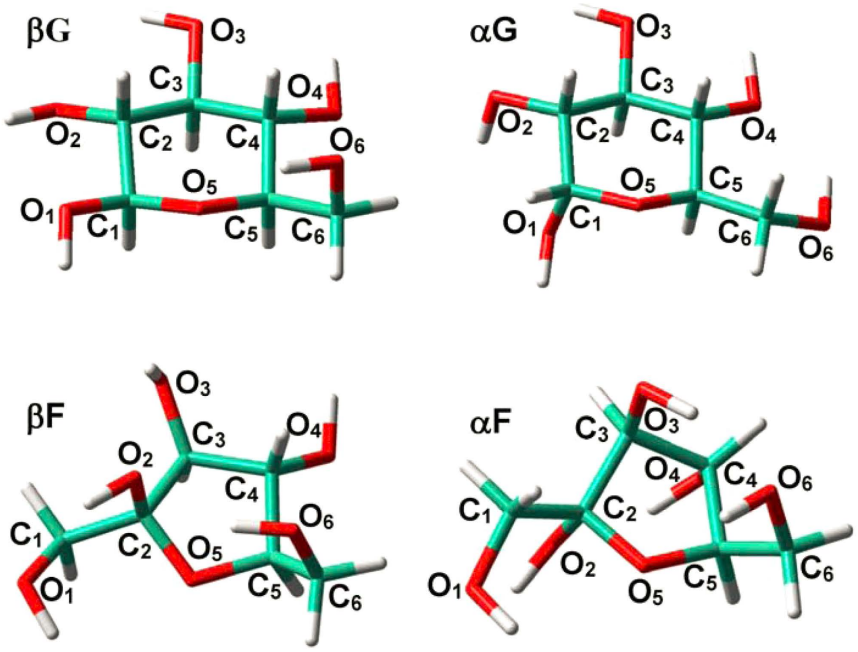

Figure 1. Structures of β-D-glucopyranose (βG), α-D-glucopyranose (αG), β-D-fructofuranose (βF) and α-D-fructofuranose (αF).

cellulosic biomass) and D-fructose (pivotal intermediate for cellulose utilization), in both α- and β-anomers, have been considered. To best of our knowledge, all previous sugar conversions focused on O sites, which are preferred over C sites during protonation[16–18,36–38] and deprotonation[20–23]. Here a systematic study was also conducted for O-centered sugar radicals, and comparisons with the results of C-centered radicals clearly indicated that the formation of C-centered radicals is always preferential, thus suggesting the possibility to activate and convert the C-H bonds of biomass sugars.

Csonka *et al.*[39] evaluated the performances of different density functionals and basis sets for the various β-D-glucose conformations. However, performances of different density functionals and basis sets for sugar radicals remain elusive, which will be conducted in this work. On such basis, the enthalpy changes and Gibbs free energies for all radicalization processes were presented with high accuracy, which can be referenced for subsequent experimental measurements. Finally, a variety of radical catalytic routes were designed and it clearly demonstrated that radicalization that focuses on activation of C sites can be used for the transformation of biomass sugars; in addition, we found that the presence of explicit water molecules can significantly alter the reaction paths and energies. These are helpful for the transformation of biomass sugars that can solve the global energy crisis.

Computational Details

In line with previous works[8–13,16–18], the lowest-energy conformers of α,β-D-glucopyranose and α,β-D-fructofuranose were the choice for studies, which were respectively referred to as **αG**, **βG** and **αF**, **βF** (Fig. 1). The various O and C sites potential to be radicalized were identified by atomic numbering; e.g., radicals corresponding to α-D-glucopyranose at O_1 site and β-D-fructofuranose at C_4 site were designated to be **αGrO$_1$** and **βFrC$_4$**, respectively. Different electronic states were considered[40,41], and radicals in doublet states that show obviously superior stabilities will be discussed unless otherwise specified.

All calculations were conducted with Gaussian09 suite of programs[42]. Structural optimizations of sugars and their radicals corresponding to the various O/C sites were performed at MP2/aug-cc-pVTZ (denoted as bs4) level[39]. The radicalization process and radical generation energies (ΔE_r) are shown as,

$$A = A^{\bullet} + H^{\bullet} \tag{2}$$

$$\Delta E_r = E(A^{\bullet}) + E(H^{\bullet}) - E(A) \tag{3}$$

Performances of other functionals and basis sets were then evaluated, using MP2/bs4 to be benchmark as suggested elsewhere[39]: 1) Hartree-Fock (HF)[43] as well as B3LYP[44,45], BP86[46], PBE1PBE[47] and M06L[48,49] density functionals, in combination with the bs4 basis set; 2) Because of relatively fine agreement with MP2 results, B3LYP was further employed with 6-31G(d), 6-31 + G(d, p) and 6-311++G(d, p) (referred to bs1, bs2, and bs3, respectively) to address the effect of basis sets; 3) Single-point energies were run at MP2/bs4 level, on basis of B3LYP optimized structures. The ΔE_r values of 1)~3) may deviate from those directly from MP2/bs4, and such deviations were defined to be $\delta\Delta E(i)$ (i being the atomic numbering of O/C site). Performances of these

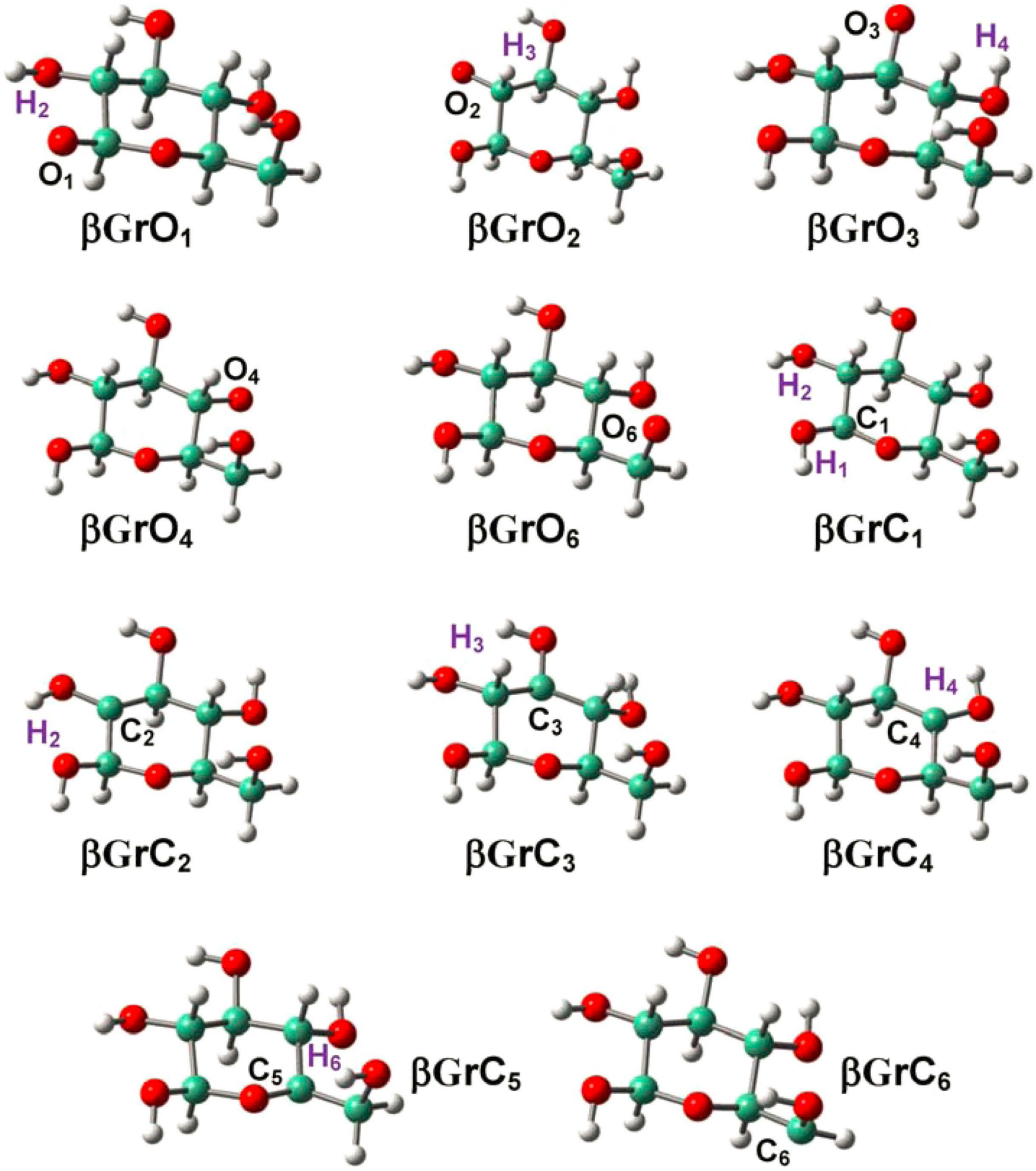

Figure 2. Optimized structures for the radicalization of β-D-glucopyranose (βG) at the various O/C sites.

functionals and basis sets can be assessed by the average of $\delta\Delta E(i)$ at the various O/C sites ($<\delta\Delta E>$) and standard deviations of $\delta\Delta E(i)$ (*S.D.*).

The enthalpy changes (ΔH) and Gibbs free energies (ΔG) for the radicalization processes can be given as[20],

$$\Delta H_r = H(A^{\bullet}) + H(H^{\bullet}) - H(A) + RT \quad (4)$$

$$\Delta G_r = \Delta H_r - T\Delta S_r = \Delta H_r - T[S(A^{\bullet}) + S(H^{\bullet}) - S(A)] \quad (5)$$

where *S*, *T* and *R* stand for entropy (in terms of tranlational, rotational and vibrational contributions), temperature and gas constant, respectively.

The thermodynamic parameters were calculated at B3LYP/bs2 level and then corrected by $\delta\Delta E(i)$, which have been testified by a large number of cases to achieve comparable results as those directly from MP2/bs4 method (Tables S1–S4 and Figures S1 and S2),

$$\Delta X(i) = \Delta X(i)^{B3LYP/bs2} + \delta\Delta E(i)\ (\Delta X = \Delta E_r, \Delta H, \Delta G, RSE) \quad (6)$$

The solvent effects were accounted for by the self-consistent isodensity polarizable continuum model (SCI-PCM) of self-consistent reaction field (SCRF)[50], in combination with B3LYP/bs2 method. The default dielectric constant ($\varepsilon = 78.4$) was used for water solvent.

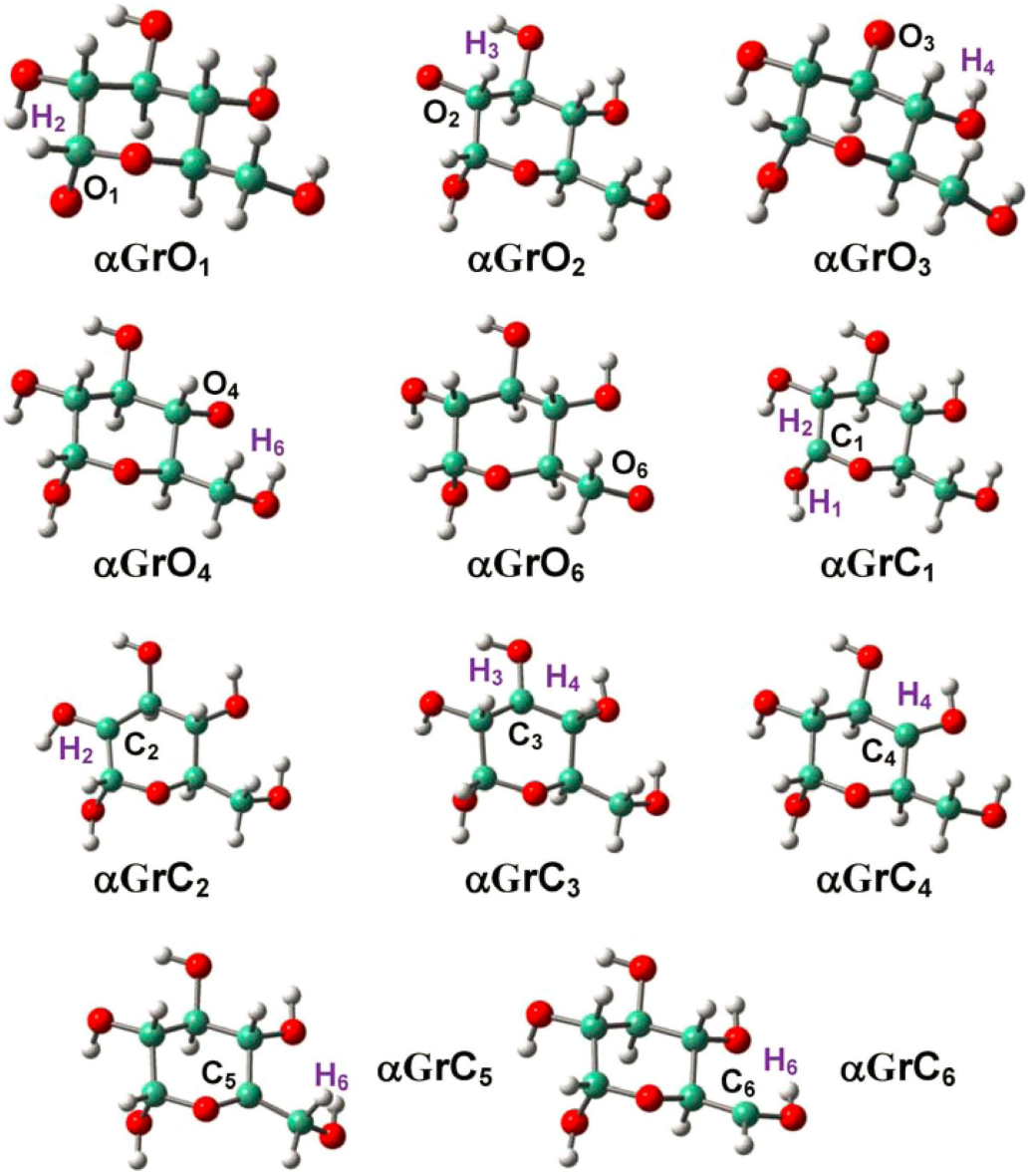

Figure 3. Optimized structures for the radicalization of α-D-glucopyranose (αG) at the various O/C sites.

For catalytic systems, the two-layer ONIOM methodology (MP2/bs4//M06L/bs3)[51,52] that has been validated sufficiently (Tables S1, S5 and Figures S3 and S4) was employed for energy calculations, on basis of B3LYP/bs2 optimized structures. The radicalized C/O sites and neighbouring C/O groups as well as adsorbents (proton and water molecules) were defined as the high-level regions, while the rest were treated as the low-level regions. This methodology can be applied for the accurate energy calculations of other sugar and larger catalytic systems.

Results and Discussion

Radicalization of D-glucopyranose. As indicated in Fig. 1, D-glucopyranose conformers (**βG** and **αG**) are inclined to construct successive H-bonds ($O_{i+1}H_{i+1}\ldots O_i$ type; e.g., $O_4H_4\ldots O_3$: 2.407 Å, $O_3H_3\ldots O_2$: 2.436 and $O_2H_2\ldots O_1$: 2.485 Å in **βG**,)[20,53]. Figures 2 and 3 show that no proton migration or ring opening occurs for the radicalization of D-glucopyranose conformers, whether at O or at C sites. Structural alterations are generally small and restricted at the radicalization sites, and two C-centered radicals previously observed during the irradiation of crystalline α-D-glucopyranose show agreement with present results[27,28,32].

Radicalization at O sites reinforces associated C-O bonds; e.g., the C_3-O_3 bonds are equal to 1.420 and 1.378 Å in **βG** and **βGrO$_3$**, respectively. The electronic densities on radicalized O atoms decline and thereby proximate H-bonds are impaired; e.g., the Mulliken charges of O_3 in **βG** and **βGrO$_3$** amount to −0.834 and −0.802, causing the elongation of $O_4H_4\ldots O_3$ H-bond from 2.407 to 2.429 Å. Radicalization at C sites strengthens the associated C-O and C-C bonds, where the pyranyl C-C/C-O bonds are apparently less affected than dangling C-O bonds; e.g., the C_2-C_3, C_3-C_4 and C_3-O_3 bonds are 1.511, 1.513 and 1.420 Å in **βG** and 1.486, 1.486 and 1.363 Å

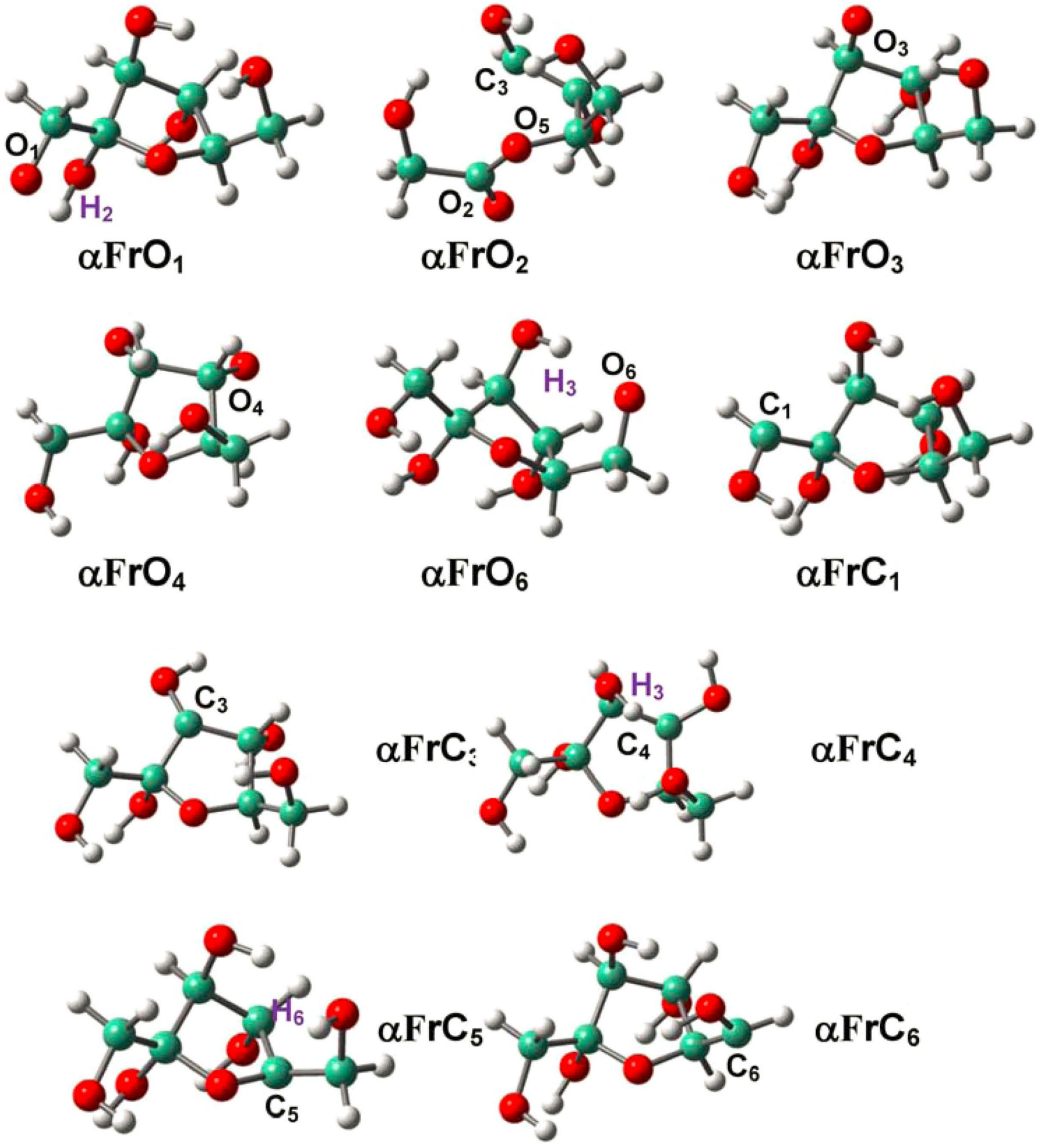

Figure 4. Optimized structures for the radicalization of α-D-fructofuranose (αF) at the various O/C sites.

in **βGrC$_3$**, respectively. The C_3-O_3 bond has been corroborated by the delocalized π-electron system developed by the lone-pair electrons of O_3 and half-empty orbital of C_3, as evidenced by electron transfers from O_3 to C_3. Whether in α- or in β-anomer, the hydroxyl (-OH) groups are alternatively up and down with respect to the pyranyl ring that are not beneficial for the formation of $O_{i+1}H_{i+1}\ldots O_i$ type H-bonds, whereas such H-bonds can be substantialized due to radicalization at C sites; e.g., the $C_2C_4C_3O_3$ dihedrals are optimized at 122.32° and 143.62° in **βG** and **βGrC$_3$**, and the larger dihedrals are in favour of $O_3H_3\ldots O_2$ and $O_4H_4\ldots O_3$ H-bonds that are 2.436 and 2.407 Å in **βG** while 2.225 and 2.367 Å in **βGrC$_3$**, respectively. C_2 site of **αG** is an exception, where the $-O_2H_2$ and $-O_1H_1$ groups fall at the same side of pyranyl ring, and radicalization elongates $O_2H_2\ldots O_1$ H-bond distance from 2.210 to 2.315 Å.

Radicalization of D-fructofuranose. Radical structures of D-fructofuranose conformers (**αF** and **βF**) are given in Figs 4 and 5. The structural alterations due to radicalization are generally local and focus on radicalization sites, which is in line with the condition of D-glucopyranose conformers[54]. Proton migration/ring opening occurs only at O_2 site of **αF**, where the furanyl ring opens by breaking C_2-C_3 bond with production of the C_2-O_2 and C_3-O_3 delocalized π-electron system.

Radicalization at O sites reinforces dangling C-O bonds and at C sites also strengthens associated furanyl C-C/C-O bonds; meanwhile, proximate H-bonds are elongated, which are consistent with the results of D-glucopyranose conformers; e.g., $O_2H_2\ldots O_1$ H-bond are 2.211 Å in **αFrO$_1$** and 2.191 Å in **αF**. However, the changing trends of H-bonds become elusive for radicalization at C sites as a result of inconsistent roles played by interlaced H-bonds: 1) Shortening as in D-glucopyranose; e.g., $O_1H_1\ldots O_5$ H-bond: 2.057 Å in **βFrC$_1$** vs. 2.602 Å in

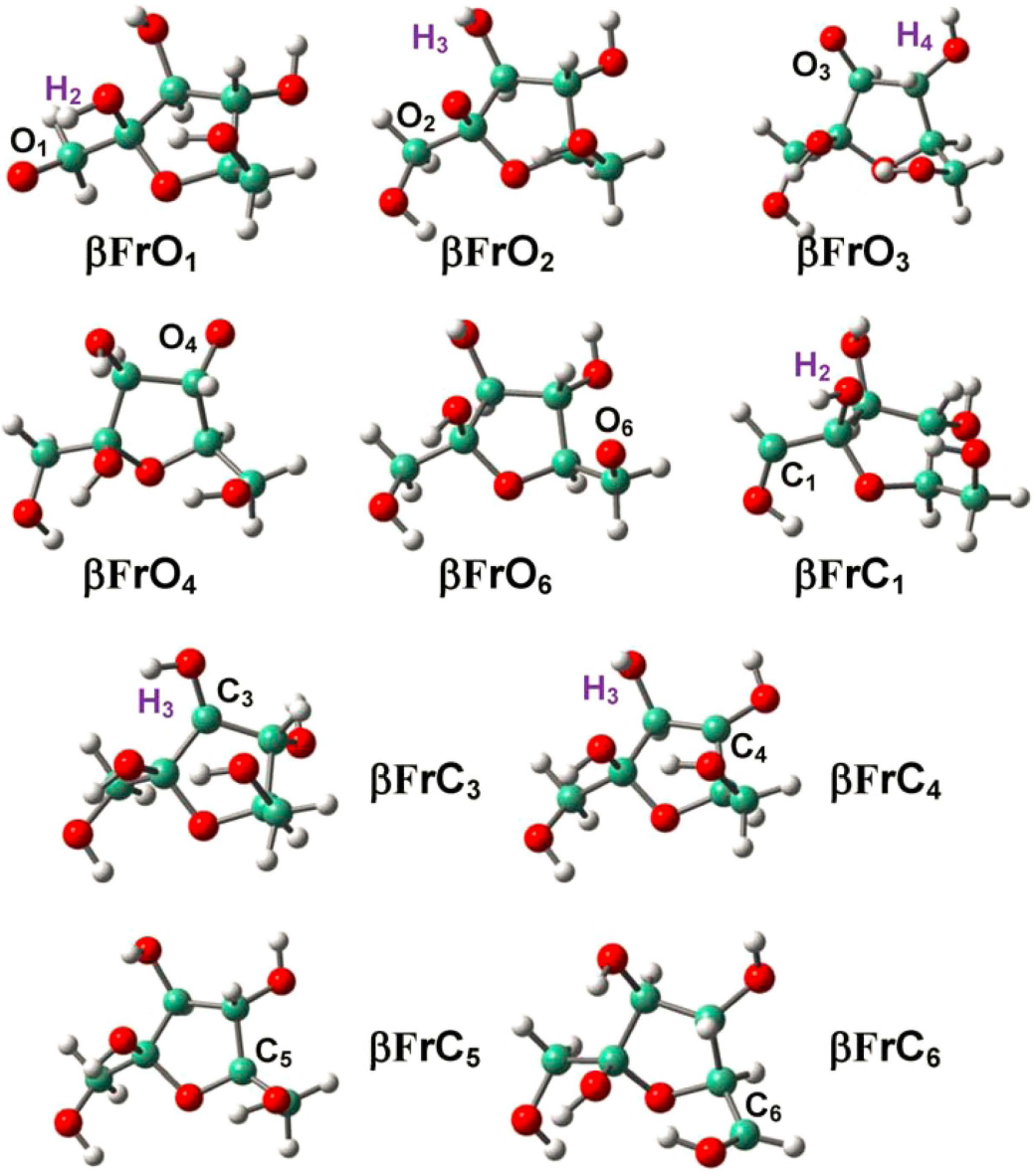

Figure 5. Optimized structures for the radicalization of β-D-fructofuranose (βF) at the various O/C sites.

	βG		αG		βF		αF	
	O	C	O	C	O	C	O	C
C_1/O_1	**495.5**	**427.3**	**500.5**	441.1	496.7	429.2	494.3	440.1
C_2/O_2	505.9	438.0	503.8	443.9	516.6		**436.4**	
C_3/O_3	506.0	429.2	506.6	431.5	505.7	430.0	500.4	440.7
C_4/O_4	506.5	427.7	510.7	431.1	497.4	428.0	504.6	**432.4**
C_5/O_5		439.8		443.1		435.1		434.1
C_6/O_6	495.8	428.6	503.1	**425.3**	502.4	**422.4**	494.5	434.7
Average	501.9	431.8	504.9	436.0	503.8	428.9	486.0	436.4

Table 1. MP2/bs4 calculated radical generation energies (ΔE_r) for D-glucopyranose and D-fructofuranose conformers at the various O/C sites[a,b]. [a]Energy units in kJ/mol. [b]In each case, the lowest radical generation energy has been highlighted in bold.

βF; 2) Apparent elongation; e.g., $O_2H_2\ldots O_1$ H-bond: 2.704 Å in **αFrC$_1$** vs. 2.191 Å in **αF**; 3) Construction of new H-bond; e.g., the $O_3H_3\ldots O_4$ H-bond: 2.449 Å in **αFrC$_3$**. Radicalization causes associated hydroxyl (-OH) groups to approach the furanyl plane; e.g., the $C_2C_4C_3O_3$ dihedrals are 118.98° and −141.97° in **αF** and **αFrC$_3$**, respectively,

	βG		αG		βF		αF	
	ΔH_r	ΔG_r	ΔH_r	ΔG_r	ΔH_r	ΔG_r	ΔH_r	ΔG_r
O_1	466.1	**381.2**	470.0	**440.8**	466.4	**437.2**	464.0	435.1
O_2	477.5	399.3	473.5	443.8	486.7	455.7	407.5	**377.1**
O_3	476.3	399.8	476.1	446.9	477.4	449.4	471.5	442.2
O_4	476.8	401.7	482.2	453.7	469.7	439.1	475.6	442.9
O_6	465.5	392.7	472.4	441.4	471.0	440.0	463.5	434.9
C_1	401.8	353.0	413.8	382.5	401.7	370.4	412.1	380.1
C_2	411.6	360.3	416.2	381.8				
C_3	403.1	**351.3**	405.1	374.1	403.6	373.4	413.6	378.2
C_4	401.4	355.7	404.8	373.9	401.3	371.7	405.3	**372.2**
C_5	413.9	358.7	415.6	380.6	408.1	373.7	407.4	374.6
C_6	401.9	359.0	398.2	**368.7**	394.9	**365.1**	407.0	377.0

Table 2. Enthalpy changes (ΔH_r) and Gibbs free energies (ΔG_r) for the radicalization of D-glucopyranose and D-fructofuranose conformers[a,b]. [a]Energy units in kJ/mol. [b]In each case, the lowest ΔG_r value has been highlighted in bold.

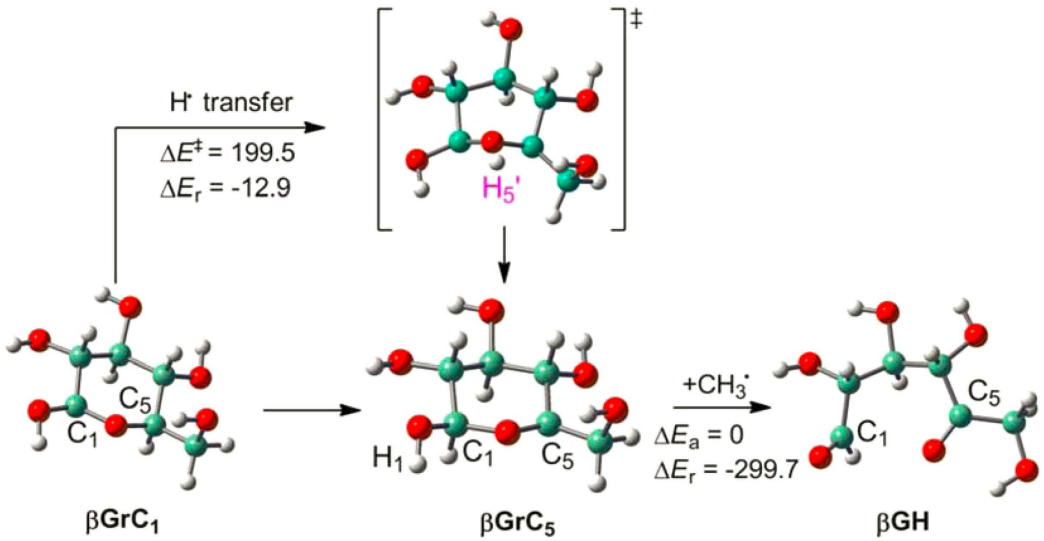

Figure 6. Illustration of catalytic transformation of C-centered sugar radicals. Energy calculations (kJ/mol) are reported at MP2/bs4//B3LYP/bs2 level. Deprivation of H radical ($H^{\bullet}$) is realized with the reaction of $\beta\mathbf{GrC_5} + CH_3^{\bullet} \rightarrow \beta\mathbf{GH} + CH_4$.

No.	Chemical formula	*RSE*	ΔE_r	ΔE_{pro}	ΔE_{deh}
				−13.3	75.2
R1	$H_3C^{\bullet}$	0	−381.0	−52.9	51.7
R2	$(CH_3)_3C^{\bullet}$	−55.4	−302.6	−89.4	53.6
R3	$CH_2{=}CHCH_2^{\bullet}$	−84.2	−295.7	−53.5	47.0
R4	$C_6H_5^{\bullet}$ (phenyl)	10.9	−399.5	−85.8	46.7
R5	$CH_3C^{\bullet}{=}O$ (acetyl)	−77.8	−325.9	−44.6	91.8
R6	$OH^{\bullet}$	35.3	−439.2	−46.4	31.2
R7	$Cl^{\bullet}$	−24.0	−364.2	10.8	52.4
R8	$H_2N^{\bullet}$	−1.7	−388.2	−140.0	47.7

Table 3. ONIOM(MP2/bs4//M06L/bs3)//B3LYP/bs2 calculated energies for the radical catalysis of $\beta\mathbf{GrC_1}$[a,b]. [a]Energy units in kJ/mol. [b]Data of the first line are for βG.

and consequently, $HO_3H_3\ldots O_6$ H-bond is damaged by radicalization of **αF** at C_3 site, and the $-O_3H_3$ group shifts to the other side of furanyl ring and creates $O_3H_3\ldots O_4$ H-bond. That is, radicalization at C sites in D-fructofuranose rather than D-glucopyranose conformers result in more pronounced effects on proximate H-bonds.

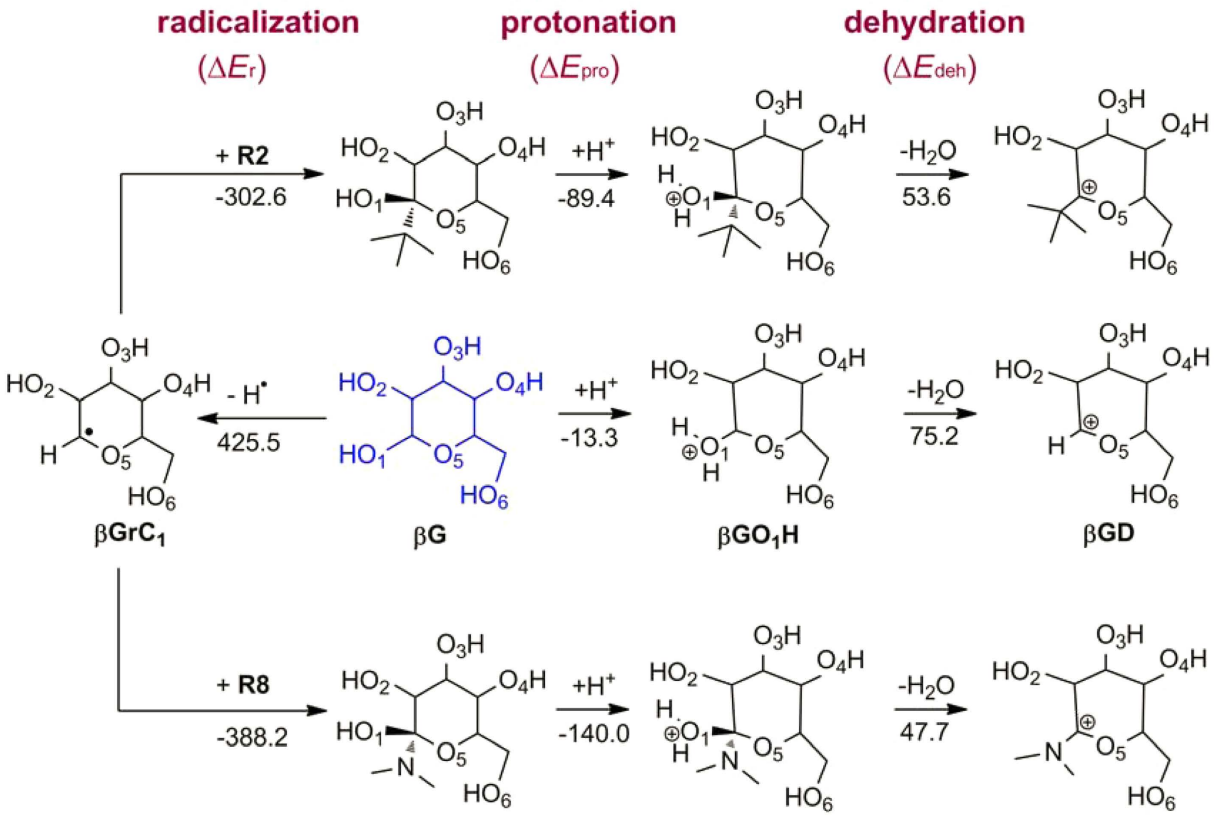

Figure 7. Regulation of catalytic effects of sugars by radical functionalization. Energy calculations (kJ/mol) are reported at ONIOM(MP2/bs4:M06L/bs3)//B3LYP/bs2 level. High-level regions are displayed in ball and stick while low-level regions in stick.

Thermodynamic Calculations. The ΔE_r and *RSE* values of sugars (**βG**, **αG**, **βF** and **αF**) corresponding to the various O/C sites are calculated at MP2/bs4 level (Tables 1 and S4). Eqs 1 and 3 show that they can be correlated with each other,

$$\Delta E_r = RSE + \text{Constant} \quad (7)$$

Accordingly, ΔE_r and *RSE* have exactly the same changing trends. The ΔE_r data of D-glucopyranose and D-fructofuranose can be comparable, and for each sugar (**βG**, **αG**, **βF** and **αF**), the ΔE_r values corresponding to the various O/C sites are close to each other, and C rather than O sites are preferred for radicalization, which is consistent with the experimental observations[27–32]. In addition, the ΔE_r data of two anomers (α/β) can differ substantially, probably as a result of anomeric effects and H-bonding diversities[20,53].

As indicated in Figure S1 and Table S1, density functional methods are apparently superior to HF for treatment of radical sugars and obtain close results as MP2. Then B3LYP, currently one of the most used density functionals, is combined with different basis sets to demonstrate the effect of basis sets. It shows that bs2 and bs3 achieve comparable results with bs4 while bs1 deviates significantly (Figure S2 and Table S1), suggesting that diffuse functions are necessary for treating sugar radicals.

Balancing the compositional cost and accuracy, B3LYP/bs2 is selected for further studies, and a number of cases in Tables S2 and S3 demonstrate that the ΔH and ΔG data calculated at B3LYP/bs2 level deviate remarkably from those of MP2/bs4, while those corrected by energy deviations ($\delta\Delta E(i)$) are also reproducible. G4MP2 is probably the most familiar composite method for energy calculations[55], and other composite methods with zero-point vibrational energies being computed at lower theoretical levels have also been reported[56,57]. The ΔH and ΔG data for radicalization of sugars at the various O/C sites are calculated this way and collected in Table 2. The lowest ΔH_r and ΔG_r values for O sites are 466.1 (O_1) and 381.2 (O_1) kJ/mol for **βG**, 470.0 (O_1) and 440.8 (O_1) kJ/mol for **αG**, 466.4 (O_1) and 437.2 (O_1) kJ/mol for **βF** and 407.5 (O_2) and 377.1 (O_2) kJ/mol for **αF** while for C sites are 401.4 (C_4) and 351.3 (C_3) kJ/mol for **βG**, 398.2 (C_6) and 368.7 (C_6) kJ/mol for **αG**, 394.9 (C_6) and 365.1 (C_6) kJ/mol for **βF** and 405.3 (C_4) and 372.2 (C_4) kJ/mol for **αF**, respectively. The radical structure of **αG** at C_6 site has been identified before[32], and this coincides well with the present results that **αGrC$_6$** has the lowest ΔH_r and ΔG_r values. The comprehensive thermodynamic parameters given in Table 2 can be referenced for subsequent experimental measurements. Solvent effects are further included for the calculations of ΔH and ΔG, and it shows that these thermodynamic parameters are affected slightly by addition of water solvent (Tables 2 and S6).

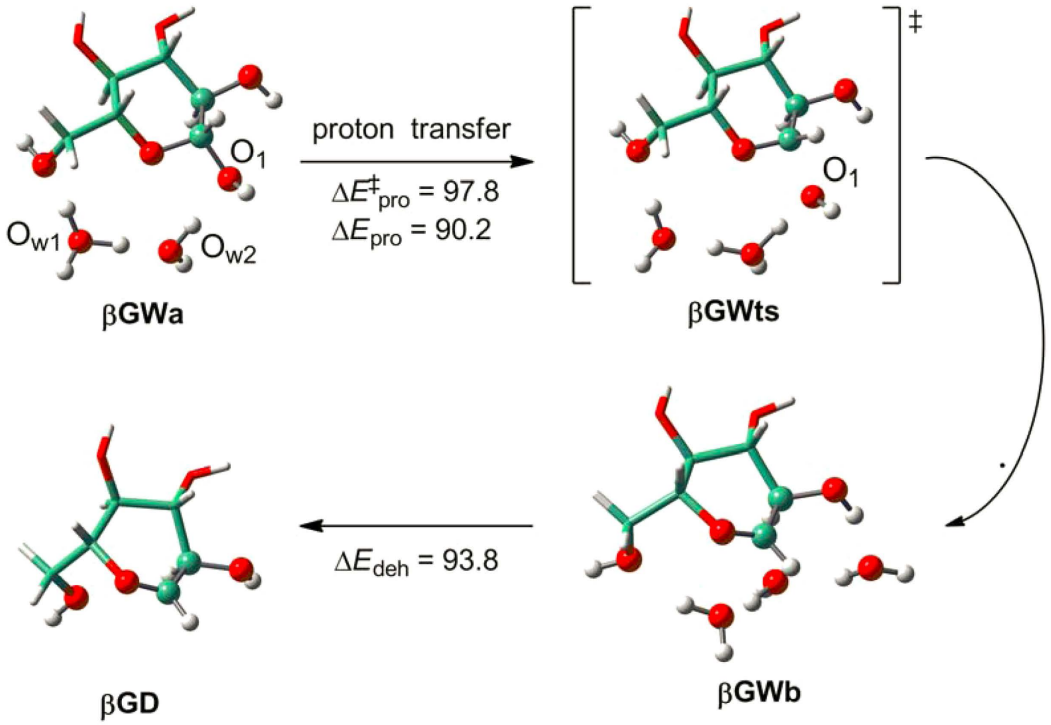

Figure 8. Protonation and dehydration of the O_1 site in β-D-glucopyranose (βG) in presence of explicit water molecules. Energy calculations (kJ/mol) are reported at ONIOM(MP2/bs4:M06L/bs3)//B3LYP/bs2 level. High-level regions are displayed in ball and stick while low-level regions in stick.

No.	chemical formula	$\Delta E^{\ddagger}_{pro}$	ΔE_{pro}	ΔE_{deh}
		97.8	90.2	93.8
R1	$H_3C^{\bullet}$	80.0	36.2	92.0
R2	$(CH_3)_3C^{\bullet}$	35.5	15.5	84.7
R3	$CH_2=CHCH_2^{\bullet}$	84.4	46.5	85.3
R4	$C_6H_5^{\bullet}$ (phenyl)	88.8	13.2	81.9
R5	$CH_3C^{\bullet}=O$ (acetyl)	131.3	90.3	83.9
R6	$OH^{\bullet}$	74.1	0.9	117.9
R7	$Cl^{\bullet}$	111.9	84.6	93.0
R8	$H_2N^{\bullet}$	30.9	−55.7	97.6

Table 4. ONIOM(MP2/bs4//M06L/bs3)//B3LYP/bs2 calculated energies for the radical catalysis of βGrC_1 in presence of two water molecules[a,b]. [a]Energy units in kJ/mol. [b]Data of the first line are for βG.

Radical Catalysis. As discussed earlier, for each sugar (**βG**, **αG**, **βF** and **αF**), the most preferential site for radicalization is always at C sites; that is, radicalization is particular by offering a route to activate the C-H bonds in sugars, in contrast to previous attempts focusing on catalysis of O sites. In addition, the ΔE_r data of C sites in D-glucopyranose and D-fructofuranose conformers are close to each other suggesting a comparable reactivity, and this provides insightful clues to the direct catalytic transformation of D-glucose instead of using D-fructose as the immediate product as widely recommended[2,7–13,19].

Thermodynamic calculations in Section 3.3 require structural optimizations at MP2/bs4 level that is computationally costly and seems not appropriate for catalytic studies. Here an alternative method is used: two-layer ONIOM(MP2/bs4//M06L/bs3) energies are calculated on basis of B3LYP/bs2 optimized structures. Tables S1, S5 and Figures S3 and S4 show that the alternative obtains comparable ΔE_r and *RSE* data as the method in Section 2; in addition, this methodology can be safely applied for the accurate energy calculations of other sugar and larger catalytic systems. Figure 6 gives an example for the direct radical transformation of sugars. The conversion from βGrC_1 to βGrC_5 through H-radical ($H^{\bullet}$) transfer requires an overwhelmingly large activation barrier ($\Delta E_a = 199.5$ kJ/mol) that is difficult to proceed at ambient conditions; however, the direct radical transformation of βGrC_5 is facile, and the $H^{\bullet}$-deprivation reaction ($\beta GrC_5 + CH_3^{\bullet} \rightarrow \beta GH + CH_4$) is barrierless, which is further driven by the high exothermicity ($\Delta E_r = -299.7$ kJ/mol). In **βGH**, the pyranyl ring is opened with emergence of two functional groups ($-C_1H=O$ and $-C_5=O$) that are ready for the future chemical synthesis.

A variety of functional groups can be implanted by radical catalysis[26,58], see Table 3. The reaction energies of **R1**~**R8** with **βGrC$_1$** (ΔE_r) are calculated at ONIOM(MP2/bs4//M06L/bs3)//B3LYP/bs2 level and affected pronouncedly by the radical stabilities: ΔE_r generally has the opposite trend as *RSE* (Table 3). Functionalized sugars are then combined with Brønsted acids to drive cellulosic sugars to downstream products. For the Brønsted-acid catalysis of D-glucopyranose, the initial protonation and dehydration steps are considered to be rate-determining[16,59], and these two steps are depicted in Fig. 7. In line with the previous work[16], the Brønsted acid is modeled as Zundel complex $H_5O_2^+$ (an approximation of proton in water), and hence the protonation energy (ΔE_{pro}) is defined as,

$$\Delta E_{pro} = E(A - H^+) + E(H_4O_2) - E(A) - E(H_5O_2^+) \quad (8)$$

With regard to **βG**, the protonation (ΔE_{pro}) and dehydration (ΔE_{deh}) energies are equal to −13.3 and 75.2 kJ/mol, respectively. As indicated in Table 3 and Fig. 7, both of ΔE_{pro} and ΔE_{deh}, especially the former, are affected significantly by functionalization; e.g., the protonation step becomes very favourable for **R8** ($H_2N^\bullet$, $\Delta E_{pro} = -140.0$ kJ/mol), while **R7** ($Cl^\bullet$) causes this step to be unfavourable ($\Delta E_{pro} = 10.8$ kJ/mol). That is, the catalytic effects of cellulosic sugars can be fundamentally regulated by functionalization.

Figure 8 shows the protonation (ΔE_{pro}) and dehydration (ΔE_{deh}) processes of **βG** in presence of two explicit water molecules. Protonation of **βG** at O_1 site causes the formation of one additional water molecule, and this step is thermodynamically unfavorable ($\Delta E_{pro} = 90.2$ kJ/mol) with a moderate activation barrier ($\Delta E^{\ddagger}_{pro} = 97.8$ kJ/mol). The protonation and dehydration processes of **βG** with different functional groups (**R1**~**R8**) are also calculated and the results are given in Table 4 and Figures S5–S12. It indicates that functionalization affects significantly the activation barriers and reaction energies of the protonation steps. For **R5**, O_1H constructs strong H-bonding with the acetyl O atom (1.772 Å, see Figure S9), and this adds the difficulty of protonation resulting in a considerably large activation barrier ($\Delta E^{\ddagger}_{pro} = 131.3$ kJ/mol). The protonation thermodynamics can be significantly driven by the functional groups with more steric hindrances (e.g., **R2**, **R4** > **R1**, **R3** > $H^\bullet$ in **βG**) or by the high stabilities of protonation products (**R6** and **R8**). In the case of **R6**, the protonation product is stabilized pronouncedly by two strong H-bonds ($O_2H_2 \cdots O_1$: 2.062 Å and $O_7H_7 \cdots O_1$: 1.469 Å, see Figure S10). In contrast, the reaction energies of dehydration seem not to be much affected by different functional groups, which are generally around 90.0 kJ/mol except **R6** corresponding to the particularly stable protonation product ($\Delta E_{deh} = 117.9$ kJ/mol).

References

1. Mäki-Arvela, P., Simakova, I. L., Salmi, T. & Murzi. D. Y. Production of lactic acid/lactates from biomass and their catalytic transformations to commodities. *Chem. Rev.* **114,** 1909–1971 (2014).
2. Bermejo-Deval, R. *et al.* Metalloenzyme-like catalyzed isomerizations of sugars by Lewis acid zeolites. *Proc. Natl. Acd. Sci. USA* **109,** 9727–9732 (2012).
3. Holm, M. S., Saravanamurugan, S. & Taarning, E. Conversion of sugars to lactic acid derivatives using heterogeneous zeotype catalysts. *Science* **328,** 602–605 (2010).
4. Caratzoulas, S. *et al.* Challenges of and insights into acid-catalyzed transformations of sugars. *J. Phys. Chem. C* **118,** 22815–22833 (2014).
5. Zhao, H. B., Holladay, J. E., Brown, H. & Zhang, Z. C. Metal chlorides in ionic liquid solvents convert sugars to 5-hydroxymethylfurfural. *Science* **316,** 1597–1600 (2007).
6. Hu, S. Q., Zhang, Z. F., Song, J. L., Zhou, Y. X. & Han, B. X. Efficient conversion of glucose into 5-hydroxymethylfurfural catalyzed by a common Lewis acid $SnCl_4$ in an ionic liquid. *Green Chem.* **11,** 1746–1749 (2009).
7. Moliner, M., Román-Leshkov, Y. & Davis, M. E. Tin-containing zeolites are highly active catalysts for the isomerization of glucose in water. *Proc. Natl. Acd. Sci. USA* **107,** 6164–6168 (2010).
8. Pidko, E. A., Degirmenci, V., van Santen, R. A. & Hensen, E. J. M. Glucose activation by transient Cr^{2+} dimers. *Angew. Chem. Int. Ed.* **49,** 2530–2534 (2010).
9. Bermejo-Deval, R. *et al.* Metalloenzyme-like catalyzed isomerizations of sugars by Lewis acid zeolites. *Proc. Natl. Acd. Sci. USA* **109,** 9727–9732 (2012).
10. Yang, G., Pidko, E. A. & Hensen, E. J. M. The mechanism of glucose isomerization to fructose over Sn-BEA zeolite: A periodic density functional theory study. *ChemSusChem* **6,** 1688–1696 (2013).
11. Rai, N., Caratzoulas, S. & Vlachos, D. G. Role of Silanol group in Sn-Beta zeolite for glucose isomerization and epimerization reactions. *ACS Catal.* **3,** 2294–2298 (2013).
12. Li, Y. P., Head-Gordon, M. & Bell, A. T. Analysis of the reaction mechanism and catalytic activity of metal-substituted beta zeolite for the isomerization of glucose to fructose. *ACS Catal.* **4,** 1537–1545 (2014).
13. Chethana, B. K. & Mushrif, S. H. Brønsted and Lewis acid sites of Sn-beta zeolite, in combination with the borate salt, catalyze the epimerization of glucose: A density functional theory study. *J. Catal.* **323,** 158–164 (2015).
14. Christianson, J. R., Caratzoulas, S. & Vlachos, D. G. Computational insight into the effect of Sn-beta Na exchange and solvent on glucose isomerization and epimerization. *ACS Catal.* **5,** 5256–5263 (2015).
15. Atanda, L. *et al.* Direct production of 5-hydroxymethylfurfural via catalytic conversion of simple and complex sugars over phosphated TiO_2. *ChemSusChem* **8,** 2907–2916 (2015).
16. Yang, G., Pidko, E. A. & Hensen, E. J. M. Mechanism of Brønsted acid catalyzed conversion of carbohydrates. *J. Catal.* **295,** 122–132 (2012).
17. Qian, X. H., Nimlos, M. R., Davis, M., Johnson, D. K. & Himmel, M. E. Ab initio molecular dynamics simulations of β-D-glucose and β-D-xylose degradation mechanisms in acidic aqueous solution. *Carbohydrate Res.* **340,** 2319–2327 (2005).
18. Qian, X. H., Johnson, D. K., Himmel, M. E. & Nimlos, M. R. The role of hydrogen-bonding interactions in acidic sugar reaction pathways. *Carbohydrate Res.* **345,** 1945–1951 (2010).
19. Nikolla, E., Román-Leshkov, Y., Moliner, M. & Davis, M. E. "One-pot" synthesis of 5-(hydroxymethyl)furfural from carbohydrates using Tin-beta zeolite. *ACS Catal.* **1,** 408–410 (2011).
20. Salpin, J. Y. & Tortajada, J. Gas-phase acidity of D-glucose. A density functional theory study. *J. Mass Spectrom.* **39,** 930–941 (2004).
21. Feng, S. T., Bagia, C. & Mpourmpakis, G. Determination of proton affinities and acidity constants of sugars. *J. Phys. Chem. A* **117,** 5211–5219 (2013).
22. Woods, R. J., Szarek, W. A. & Vedene, H. S., Jr. The proton affinities and deprotonation enthalpies of D-fructopyranose and L-sorbopyranose. *Can. J. Chem.* **69,** 1917–1928 (1991).

23. Flosadottir, H. D., Bald, I. & Ingólfsson, O. Fast and metastable fragmentation of deprotonated D-fructose - A combined experimental and computational study. *Int. J. Mass Spectrom.* **305,** 50–57 (2011).
24. Liu, C. *et al.* Selective base-catalyzed isomerization of glucose to fructose. *ACS Catal.* **4,** 4295–4298 (2014).
25. Mukherjee, S. & List, B. Organic chemistry: Radical catalysis. *Nature* **447,** 152–153 (2007).
26. Studer, A. & Curran, D. P. Catalysis of radical reactions: A radical chemistry perspective. *Angew. Chem. Int. Ed.* **55,** 58–102 (2016).
27. Vanhaelewyn, G. *et al.* Electron magnetic resonance study of stable radicals in irradiated D-fructose single crystals. *Phys. Chem. Chem. Phys.* **3,** 1729–1735 (2001).
28. Pauwels, E., van Speybroeck, V. & Waroquier, M. Radiation-induced radicals in α-D-glucose: Comparing DFT cluster calculations with magnetic resonance experiments. *Spectrochim. Acta Part A* **63,** 795–801 (2006).
29. Tarpan, M. A., Pauwels, E., Vrielinck, H., Waroquier, M. & Callens, F. Electron magnetic resonance and density functional theory study of room temperature X-irradiated D-fructose single crystals. *J. Phys. Chem. A* **114,** 12417–12426 (2010).
30. Kusakovskij, J., Callens, F. & Vrielinck, H. EMR study and DFT-assisted identification of transient radicals in X-irradiated crystalline sucrose. *J. Phys. Chem. B* **119,** 6562–6570 (2015).
31. Pauwels, E. *et al.* Tentative structures for the radiation-induced radicals in crystalline β-D-fructose using density functional theory. *J. Phys. Chem. A* **106,** 12340–12348 (2002).
32. Declerck, R., Pauwels, E., van Speybroeck, V. & Waroquier, M. Molecular environment and temperature dependence of hyperfine interactions in sugar crystal radicals from first principles. *J. Phys. Chem. B* **112,** 1508–1514 (2008).
33. Croft, A. K., Easton, C. J. & Radom, L. Design of radical-resistant amino acid residues: A combined theoretical and experimental investigation. *J. Am. Chem. Soc.* **125,** 4119–4124 (2003).
34. Yang, G., Zu, Y. G. & Zhou, L. Deprotonation and radicalization of glycine neutral structures. J. *J. Phys. Org. Chem.* **21,** 34–40 (2008).
35. Hioe, J. & Zipse, H. Radical stability and its role in synthesis and catalysis. *Org. Biomol. Chem.* **8,** 3609–3617 (2010).
36. Jebber, K. A., Zhang, K., Cassady, C. J. & Chung-Phillips, A. Ab initio and experimental studies on the protonation of glucose in the gas phase. *J. Am. Chem. Soc.* **118,** 10515–10524 (1996).
37. Liu, D. J., Nimlos, M. R., Johnson, D. K., Himmel, M. E. & Qian, X. H. Free energy landscape for glucose condensation reactions. *J. Phys. Chem. A* **114,** 12936–12944 (2010).
38. Jadhav, H., Pedersen, C. M., Sølling, T. & Bols, M. 3-Deoxy-glucosone is an intermediate in the formation of furfurals from D-glucose. *ChemSusChem* **4,** 1049–1051 (2011).
39. Csonka, G. I., French, A. D., Johnson, G. P. & Stortz, C. A. Evaluation of density functionals and basis sets for carbohydrates. *J. Chem. Theory Comput.* **5,** 679–692 (2009).
40. Li, D. M., Huang, X. Q., Han, K. L. & Zhan, C. G. Catalytic mechanism of cytochrome P450 for 5′-hydroxylation of nicotine: Fundamental reaction pathways and stereoselectivity. *J. Am. Chem. Soc.* **133,** 7416–7427 (2011).
41. Li, D. M., Wang, Y. & Han, K. L. Recent density functional theory model calculations of drug metabolism by cytochrome P450. *Coordination Chem. Rev.* **256,** 1137–1150 (2012).
42. Gaussian 09, Revision D.01, Frisch, M.J. *et al.* Gaussian, Inc., Wallingford CT (2013).
43. Roothaan, C. C. J. New developments in molecular orbital theory. *Rev. Mod. Phys.* **23,** 69–89 (1951).
44. Becke, A. D. A Multicenter numerical integration scheme for polyatomic molecules. *J. Chem. Phys.* **88,** 2547–2551 (1988).
45. Lee, C., Yang, W. T. & Parr, R. G. Development of the Colle-Salvetti correlation energy formula into a functional of the electron density. *Phys. Rev. B* **37,** 785–789 (1988).
46. Perdew, J. P. Density-functional approximation for the correlation energy of the inhomogeneous electron gas. *Phys. Rev. B* **33,** 8822–8824 (1986).
47. Adamo, C. & Barone, V. Toward reliable density functional methods without adjustable parameters: The PBE0 model. *J. Chem. Phys.* **110,** 6158–6169 (1999).
48. Zhao, Y. & Truhlar, D. G. A new local density functional for main-group thermochemistry, transition metal bonding, thermochemical kinetics, and noncovalent interactions. *J. Chem. Phys.* **125,** 194101 (2006).
49. Zhao, Y. & Truhlar, D. G. The M06 Suite of Density functionals for main group thermochemistry, thermochemical kinetics, noncovalent interactions, excited states, and transition elements: Two new functionals and systematic testing of four M06-class functionals and 12 other functionals. *Theor. Chem. Acc.* **120,** 215–241 (2008).
50. Tomasi, J., Mennucci, R. & Cammi, R. Quantum Mechanical Continuum Solvation Models. *Chem. Rev.* **105,** 2999–3093 (2005).
51. Lundberg, M., Kawatsu, T., Vreven, T., Frisch, M. J. & Morokuma, K. Transition states in a protein environment - ONIOM QM:MM modeling of isopenicillin N synthesis. *J. Chem. Theory Comput.* **5,** 222–234 (2009).
52. Chung, L W. *et al.* The ONIOM nethod and its applications. *Chem. Rev.* **115,** 5678–5796 (2015).
53. Alonso, J. L. *et al.* The conformational behavior of free D-glucose - At last. *Chem. Sci*. **5,** 515–522 (2014).
54. Yang, G., Li, X. & Zhou, L. J. Adsorption of fructose in Sn-BEA zeolite from periodic density functional calculations. *RSC Adv*. **6,** 8838–8847 (2016).
55. Curtiss, L. A., Redfern, P. C. & Raghavachari, K. Gaussian-4 theory using reduced order perturbation theory. *J. Chem. Phys.* **127,** 124105 (2007).
56. Rankin, K. N., Gauld, J. W. & Boyd, R. J. Density functional study of the proline-catalyzed direct aldol reaction. *J. Phys. Chem. A* **106,** 5155–5159 (2002).
57. Yang, G., Yang, Z. W., Zhou, L. J., Zhu, R. X. & Liu, C. B. A revisit to proline-catalyzed aldol reaction: Interactions with acetone and catalytic mechanisms. *J. Mol. Catal. A: Chemistry* **316,** 112–117 (2010).
58. Tang, S., Liu, K., Liu, C. & Lei, A. W. Olefinic C-H functionalization through radical alkenylation. *Chem. Soc. Rev.* **44,** 1070–1082 (2015).
59. Yang, L., Tsilomelekis, G., Caratzoulas, S. & Vlachos, D. G. Mechanism of Brønsted acid-catalyzed glucose dehydration. *ChemSusChem* **8,** 1334–1341 (2015).

Acknowledgements

This work was sponsored by the National Natural Science Foundation of China (21473137) and Fourth Excellent Talents Program of Higher Education in Chongqing (2014-03) and Fundamental Research Funds for the Central Colleges (SWU113049 and XDJK2014C106).

Author Contributions

G.Y. designed the experiments and prepared the manuscript. C.Z., X.Z. and L.Z. helped analyse the results. All authors reviewed and approved the manuscript.

Additional Information

Supplementary information accompanies this paper at http://www.nature.com/srep

Competing financial interests: The authors declare no competing financial interests.

How to cite this article: Yang, G. *et al.* Radicalization and Radical Catalysis of Biomass Sugars: Insights from First-principles Studies. *Sci. Rep.* **6**, 29711; doi: 10.1038/srep29711 (2016).